CALIFORNIA STATE UNIVERSITY NORTHRIDGE

Impact of Grid Connected PV penetration on Grid

A graduate project submitted in partial fulfillment of the requirements
For the degree of Master of Science in Electrical Engineering

By
Abhishek Ayyannagari

December 2016

The graduate project of Abhishek Ayyannagari is approved:

_____	_____
Dr. Xiaojun (Ashley) Geng	Date
_____	_____
Professor Benjamin Mallard	Date
_____	_____
Dr. Kourosh Sedghisigarchi, Chair	Date

California State University Northridge

Acknowledgement

The completion of this project would not have been possible without the continuous support and feedback from Dr. Kourosh Sedghisigarchi, Dept. Of Electrical & Computer Engg., and it was my pleasure working under his guidance. I would also like to express my gratitude to the committee members Dr. Ashley Geng and Prof. Benjamin Mallard for their academic and moral support throughout the project.

Last, but not the least I would like to thank everyone who has directly or indirectly contributed to making the project a success.

Table of Contents

List of Figures

List of Tables

List of Abbreviations

PV	Photovoltaic
TWH	Tera watt hour
MM Tons	Million metric tons
DC	Direct current
AC	Alternating current
MPPT	Maximum power point tracking
SC	Short Circuit
OC	Open Circuit
LV	Low Voltage
HV	High Voltage
DNI	Direct Normal Irradiance
PU	Per Unit

Abstract

Grid Connected Photo Voltaic System

By

Abhishek Ayyannagari

Master of Science in Electrical Engineering

The generation of power at the point of consumption is referred to as DG. It can be any source with a generation capacity of 10MW or less. With increase in concerns for protection of the environment from the pollution caused by thermal plants etc., there has been a rapid increase of DG penetration into the grid. DG's are mostly renewable sources of energy like solar, wind etc. This not only reduces the pollution but helps in improving the voltage profile and power losses in the system [9, 13]. However, this causes a lot of concerns as well, such as overvoltage, system protection etc. Therefore, increases the complexity of the system. In this project, the impacts of PV system penetration for two cases with a penetration level of 5% and 10%, on a 15 Bus IEEE system in a regular summer day has been simulated.

In this system, a PV module has been developed, and the output connected to an IEEE 15 bus system through a DC-DC converter and an AC-DC inverter. The power curves at the generating buses, the voltage profile and the power loss in the system have been investigated for both the cases. The solar irradiation data for CSUN campus on a sunny summer day has been applied to the developed PV system.

Chapter 1

INTRODUCTION

In this chapter, the ever rising energy demand due to the rapid growth of population, and the need to meet the energy gap through renewable energy sources such as solar has been discussed. A brief introduction to solar energy, PV panels, and the factors effecting its performance have been detailed.

1.1 Literature Review

With the increase in demand for energy, the electrical distribution networks are undergoing rapid reorganization, to meet the demand. And one such change is the addition of DGs to the existing networks, at various locations in the system. This has both positive impacts such as improvement in the voltage profile and power losses of the system, and negative impacts such as overvoltage, reverse power flow [10] and system protection [13]. The losses and system reliability can be studied through a load flow analysis on the system [9]. The increase in the interconnection of the DGs is a cause for concern of the system protection, which is usually planned for traditional radial distribution systems [8]. The location of the DG in the system has to be optimally planned to take into account the relay coordination settings and maximum penetration into the grid without increasing the losses in the system [4].

1.2 Global Energy Scenario

The rapid increase in global energy demand and the need to reduce global warming, pollution etc. have paved way for the research and implementation of renewable energy sources such as solar, wind etc. As shown in fig. 1.1 [1], it can be observed that the electricity demand has almost doubled in the last decade. And it is estimated that, by the year 2020 the electric power consumption would reach 25.8 TWh.

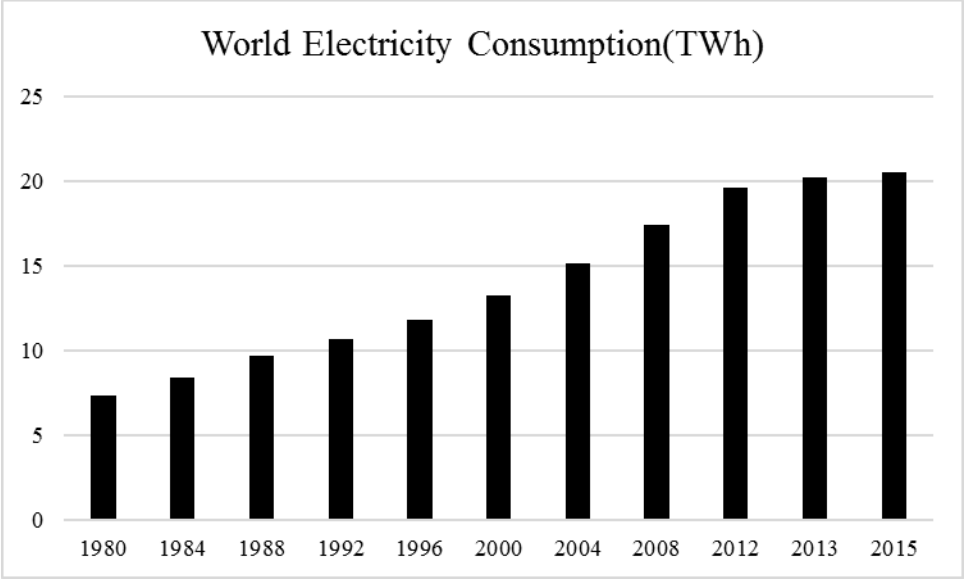

Figure 1.1: World Electricity Consumption in TWh [1]

As the rate of consumption of electricity increases, the pollution i.e. emission of carbon-dioxide into the atmosphere also increases, as can be observed from the fig. 1.2 [1], which results in global warming. To meet the ever growing demand and to minimize pollution, demand for alternate sources of energy such as solar, wind etc. has been increasing.

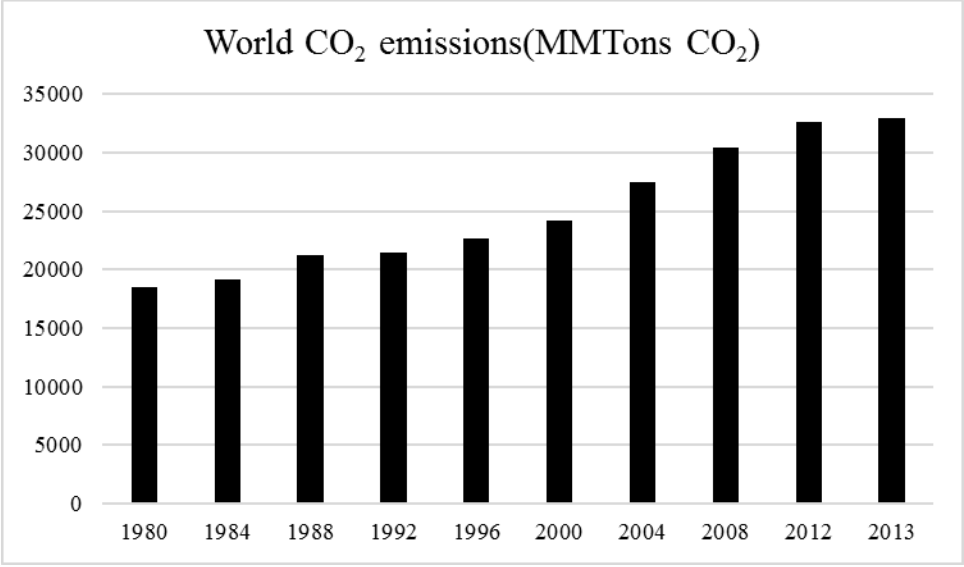

Figure 1.2: World CO_2 emissions [1]

1.3 Solar Energy

Solar energy is generation of electricity by harnessing the heat and light from the sun's rays which strike the surface of the earth during the day. The energy can be harnessed by various methods such as using PV cells, solar heating etc.

It can be observed from fig. 1.3 [1], which shows that since the start of the decade the installed capacity of PV has more than tripled. This rapid increase in the installation of solar plants is because of the year-round availability, easy forecast of solar insolation and very low maintenance costs after installation.

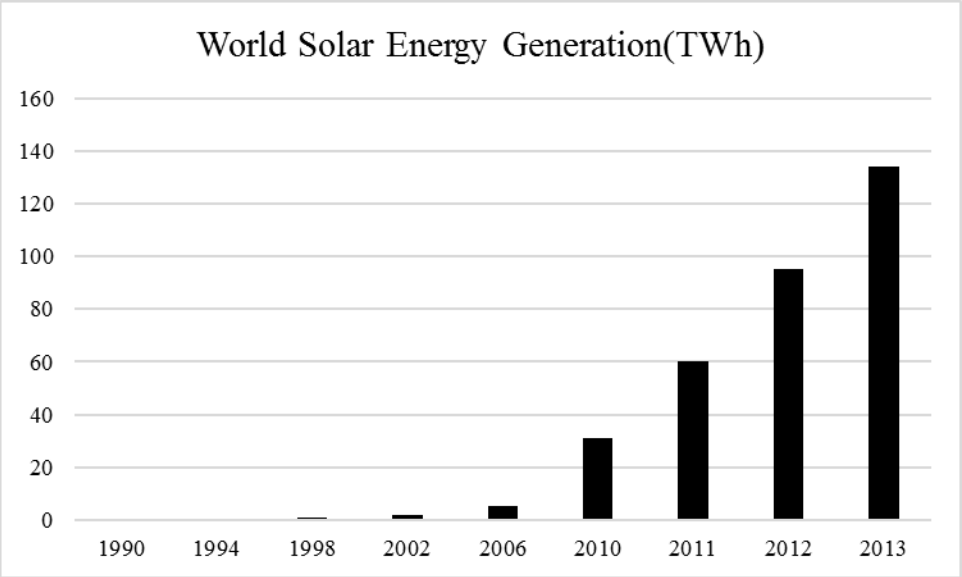

Figure 1.3: World Solar Energy Generation in TWh [1]

Chapter 2

Grid Connected PV Systems

A PV system has many components involved in order to be connected to the grid [10]. Some of these components/systems have been described in this chapter. The fig. 2.1 represents the components of a typical PV system connected to the power grid.

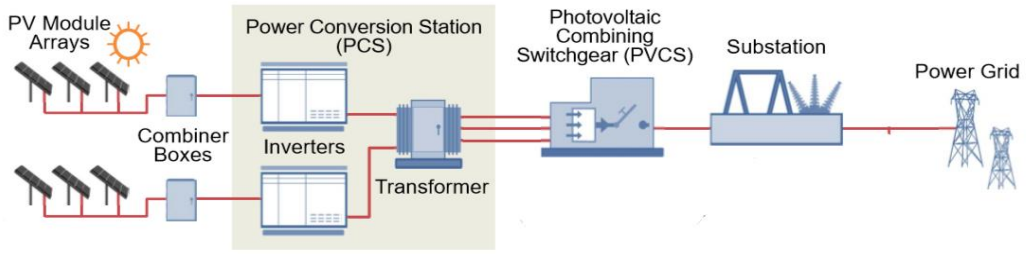

Figure 2.1: PV system connected to the grid

2.1 Photovoltaic Cells

The Photovoltaic phenomenon was first experimentally proved by a French physicist Edmond Becquerel in the year 1839, but the first practical PV cell was developed in April, 1954 by Bell Laboratories for use in satellites. Later with further research and development PV cells were made using silicon, for terrestrial applications.

The silicon layers are stacked into p-type and n-type materials, which upon striking of solar radiation generate holes and electrons, when the energy is greater than the band gap, the current is generated which is nothing but Direct Current (DC). The fig. 2.2 [2] shows the structure and working principle of a PV cell.

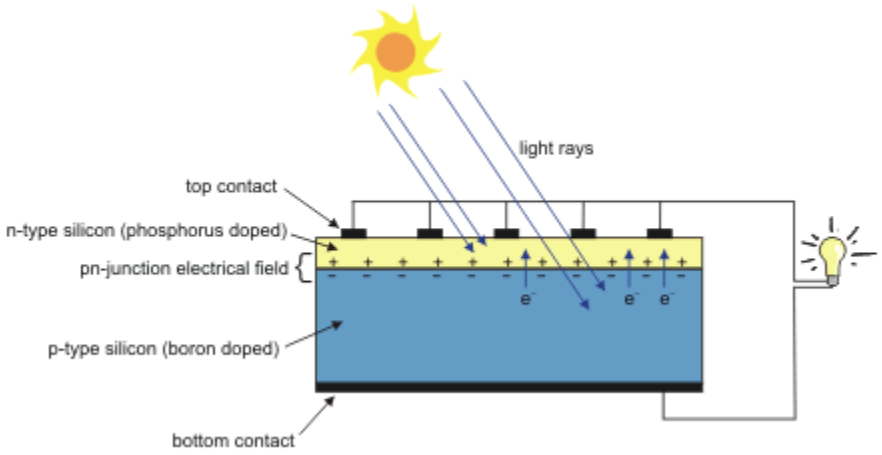

Figure 2.2: Structure and working of a PV cell [2]

The PV cells when stacked together in series/parallel to form an array/module generate sufficient power to supply various electrical appliances and home. The efficiency of a PV cell is in the range of 15-20%, depending on the type of manufacturing of the solar cell, such as thin film, mono and poly-crystalline solar panels.

However, there are various factors which affect the output of a PV cell, some of which are;

a) Insolation – It is the amount of sun's light striking the surface of the panel or a given area. The solar insolation and the output of the PV panel are directly proportional.

b) Temperature – The temperature of the PV cell plays a vital role in the power output of the PV panel. As the temperature rises the PV panel voltage decreases, thereby decreasing the generated power. Hence, areas with colder climate are preferred for installation of the PV plants.

2.2 PV Module

The PV modules in common consist of an array of PV cells usually in a 6x10 configuration. These modules depending on the manufacturing process have a wide range of efficiencies. The commercially available multi-crystalline Si PV cells have an efficiency of 14-19%, which usually generate a power of around 200W for an area of $1m^2$ of solar insolation. Usually the PV modules are rated based on the product of their open circuit voltage(V_{oc}) and the short circuit current(I_{sc}), however an accurate understanding of the PV capacity can be achieved by studying the load curves.

2.2.1 Site Selection

a) The location of the PV module must be free from the shades of trees, building or any shadows cast by nearby objects.

b) The PV module should face the sun directly for maximum performance. In the southern hemisphere the PV modules should face the north, and vice versa. For every 30^o deviation of the PV modules from the true north or south, there would be power loss of 10% to 15%.

c) For systems with constant tilt angle, the optimum tilt angle would be for winter conditions. The table 2.1 [11] specifies the tilt angle for a specific latitude.

SITE LATITUDE IN DEGREES	FIXED TILT ANGLE
0° TO 15°	15°
15° TO 25°	SAME AS LATITUDE
25° TO 30°	LATITUDE + 5°
30° TO 35°	LATITUDE + 10°
35° TO 40°	LATITUDE + 15°
40° +	LATITUDE + 20°

Table 2.1: Optimum tilt angle for fixed PV systems-based on winter performance [11]

2.2.2 Advantages

a) Solar insolation is available year round, and is a free source of energy unlike fossil fuels.

b) It can be used to set up power generating stations in remote locations, without the need for supply from a grid [12].

c) It reduces the cost of laying transmission lines from the conventional generating stations to far away locations, as it can be setup near to the load.

d) It can be constructed to any size as per the load, as it consists of modules which can be added with the increase in load every year.

e) PV systems can be setup easily on unused residential or commercial rooftops and do not cause any noise or air pollution.

f) The PV system requires very low maintenance compared to the conventional generating stations.

2.2.3 Disadvantages

a) The toxic chemicals such as arsenic and cadmium used in the manufacturing of PV panels need to be disposed or recycled very carefully to avoid harm to the environment.

b) The initial investment for setup, control, batteries and land acquisition can be challenging. [12]

c) As the solar insolation is available only during the day, it cannot be used as the primary source of energy. It has to be supplemented with a conventional energy source or the excess energy from PV must be stored in batteries for use in the night. which further increases the cost and energy losses, due to the low efficiency of the batteries.

Chapter 3

Design using MATLAB/SIMULINK

The parameters and equations to build the PV module, DC-DC converter and the IEEE 15 bus system have been described.

3.1 Photovoltaic System

In general, any PV system consists of a PV module which generates a DC output, DC-DC converter which boosts the voltage, DC-AC inverter and a transformer which increases the voltage to match the grid it is being fed into as shown in the fig. 3.1.

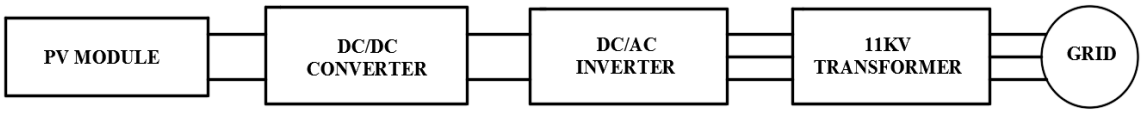

Figure 3.1: Block diagram of a PV system

3.2 PV Module

The PV cell can be modeled as an equivalent circuit consisting of the photo current source, diode, a resistance in parallel and series which represent the leakage current and the internal resistance respectively as shown in the fig. 3.2, and has been modeled in Simulink using the equations taken from reference [3].

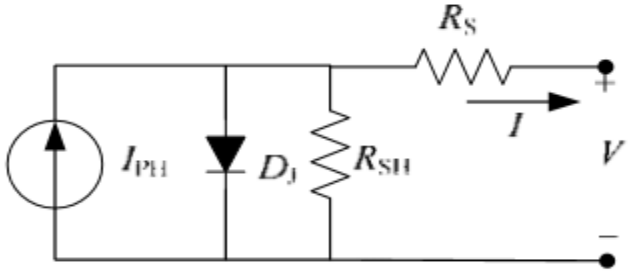

Figure 3.2: Generalized model of a PV cell [3]

Equation (1) represents the voltage-current characteristics of the PV cell;

$I = I_{ph} - I_s [\exp (q (V + I*R_s) / k*T_c*A) -1] - (V + I*R_s)/R_{sh}$ ----------(1)

Where, I_{ph} is the photocurrent

I_s is the cell saturation of dark current

q = 1.6 ×10-19C, is the charge of an electron

k = 1.38 ×10-23J/K, is the Boltzmann constant

T_c is the working temperature of the PV cell

A is the ideal factor

R_{sh} is the shunt resistance

R_s is the series resistance

The equation (2) represents the photocurrent which depends on the operating temperature of the PV cell and the solar insolation;

$I_{ph} = [I_{sc} + K_i*(T_c*T_{ref})]*\lambda$ ----------(2)

Where, I_{sc} is the short-circuit current of the cell at a 25°C

K_i is the short-circuit current temperature coefficient of the cell

T_{ref} is the reference temperature of the cell

λ is the solar insolation in kW/m^2.

The cell's saturation current varies with the cell temperature, which is described as;

$I_s=I_{rs}*(T_c /T_{ref})^3\{\exp [q*E_g*(1/T_{ref} -1/T_c)/ k*A]\}$ ----------(3)

Where, I_{rs} is the reverse saturation current of the cell at the reference temperature and solar radiation

E_g is the bang-gap energy of the semiconductor material used in the cell.

The open-circuit voltage $V_{oc,}$ is calculated by assuming that the output current is zero. Now, the reverse saturation current at the reference temperature can be obtained by using the equation (4);

$I_{rs} = I_{sc} / [\exp (q*V_{oc}/(N_s*k*A*Tc))-1]$ ----------(4)

Where, N_s is the no. of PV cells

PV panel specifications:

Model	Kyocera-KC200GT
V_{oc}	32.9 Volts
I_{sc}	8.21 Amps
No. of Cells (N_s)	54
K_i	0.003
Ideal Factor for Si (A)	1.3
Band-gap Energy (E_g)	1.11

Table 3.1: PV panel specifications

The fig. 3.3 shows the Simulink model of the PV cell;

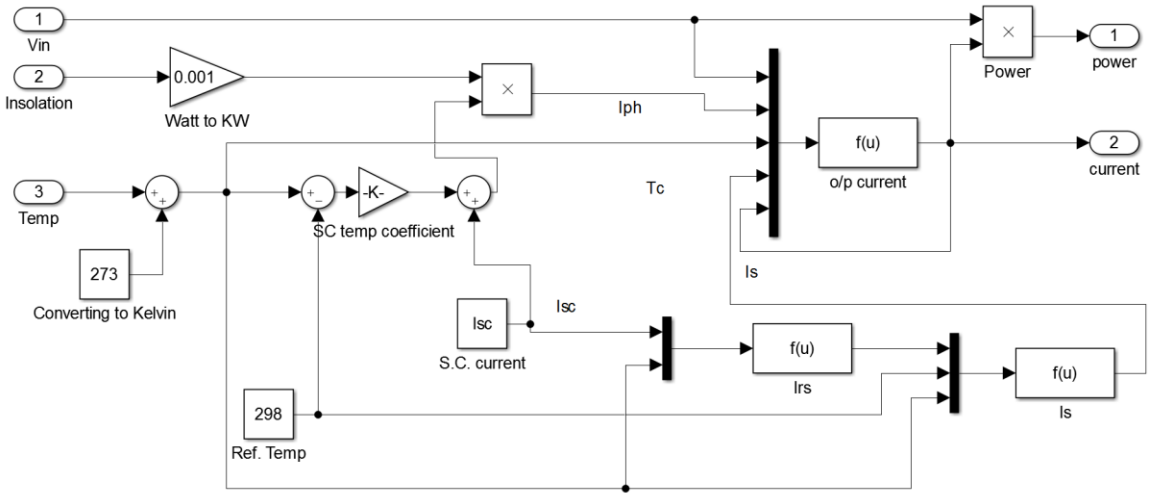

Figure 3.3: PV cell Simulink model

The solar irradiation and temperature have been obtained for a particular sunny day April, 2nd, 2015 for the Northridge, California location from [6] which has been shown in the fig. 3.4.

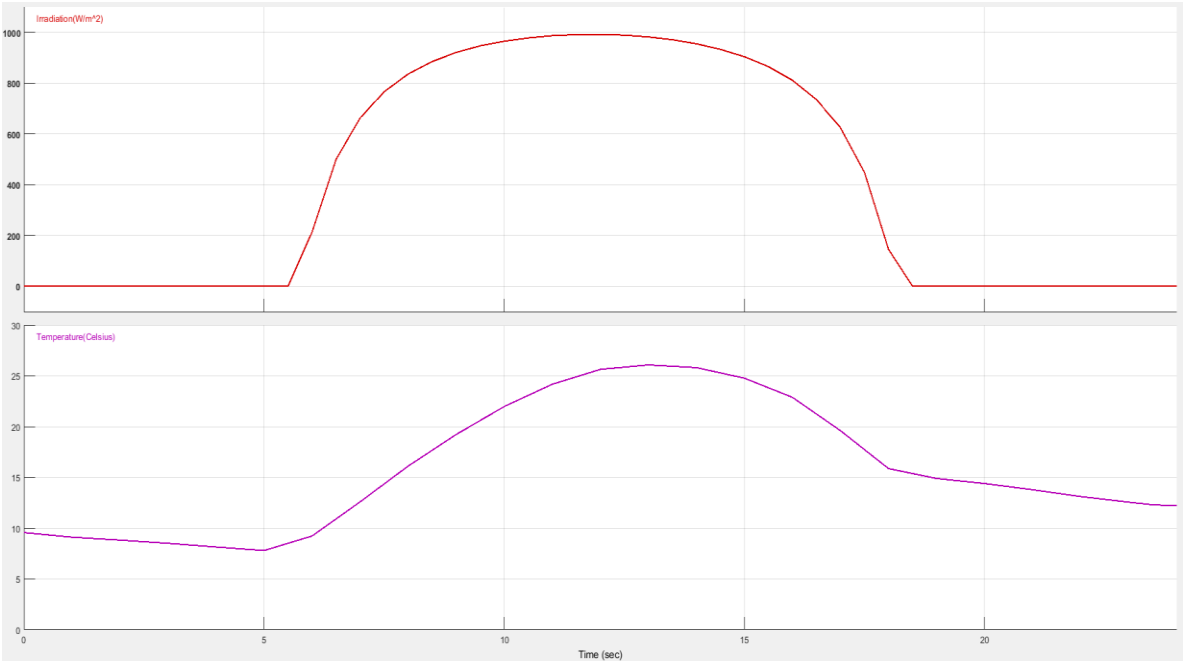

Figure 3.4: Solar irradiation and temperature

3.3 DC-DC Converter

The DC-DC boost converter [7] boosts the voltage of the PV module, i.e. the output voltage obtained from the boost converter, can be more than the input voltage, which depends on the operation of the MOSFET which acts as a switch at a very high frequency to generate a chopped voltage. This process decreases the current, to increase the voltage so that the power is constant.

The MPPT controller is based on the perturbation and observation [5] algorithm, which adjusts the duty cycle for the maximum power point of the PV output. The flowchart of the algorithm is as shown in the fig. 3.5.

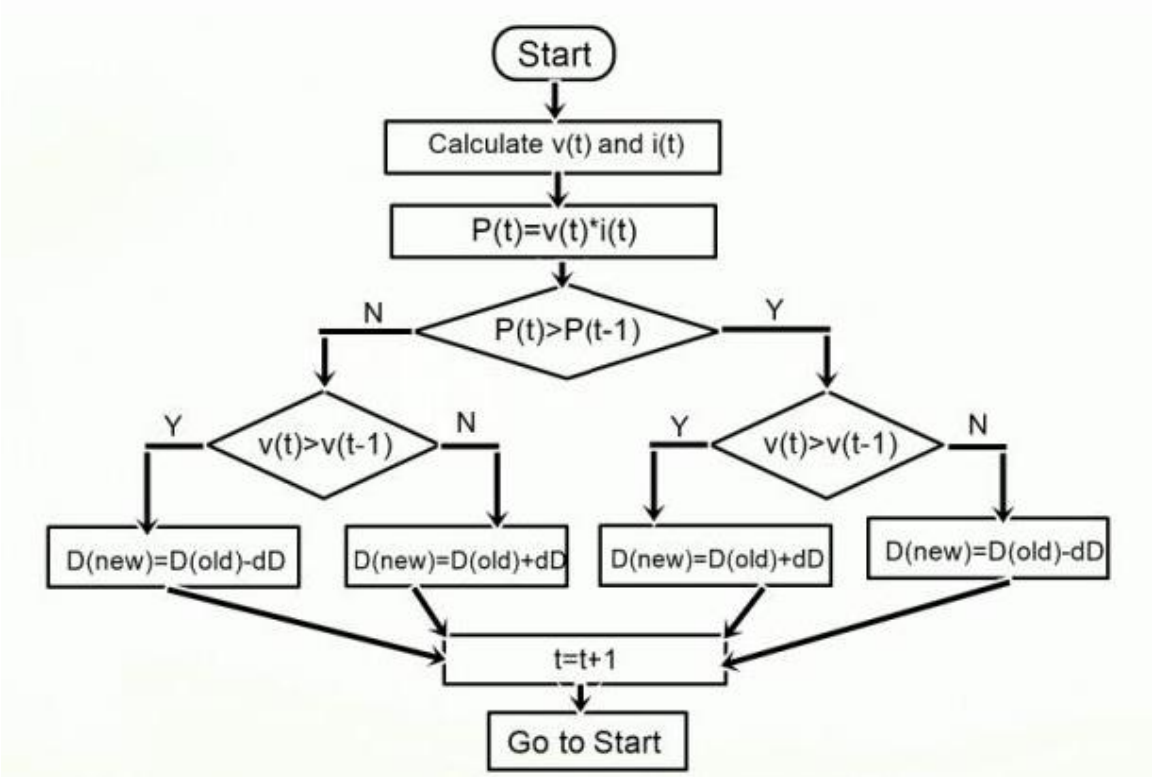

Figure 3.5: Perturbation & Observation Flowchart [7]

The perturbation and observation method is implemented using the matlab code block in Simulink and the code is as shown in the fig. 3.6 [5].

```
function D  = PandO(V, I)

% MPPT controller based on the Perturb & Observe algorithm.
% D output = Duty cycle of the boost converter
% V input = PV voltage (V)
% I input = PV current (A)

Dinit = 0.5;  %Initial value for D output
Dmax = 0.58;   %Maximum value for D
Dmin = 0.38;   %Minimum value for D
deltaD = 0.0003;%Increment value used to increase/decrease the dutycycle D

persistent Vold Pold Dold;

dataType = 'double';

if isempty(Vold)
    Vold=0;
    Pold=0;
    Dold=Dinit;
end
P= V*I;
dV= V - Vold;
dP= P - Pold;

if dP ~= 0
    if dP < 0
        if dV < 0
            D = Dold - deltaD;
        else
            D = Dold + deltaD;
        end
    else
        if dV < 0
            D = Dold + deltaD;
        else
            D = Dold - deltaD;
        end
    end
else D=Dold;
end

if D >= Dmax | D<= Dmin
    D=Dold;
end

Dold=D;
Vold=V;
Pold=P;
```

Figure 3.6: Perturbation & Observation code [5]

The table 3.2 shows the values of the capacitors, inductor and resistor.

Parameters	Value
C1	0.0001 farad
L	0.1 henry
C2	0.012 farad
R	500 ohms

Table 3.2: Values of R, L, C

3.4 DC-AC Inverter

The inverter converts the DC output from the DC-DC converter to three phase AC to be fed to the grid through a 11kV transformer. The fig. 3.7 shows the settings of the three phase inverter block.

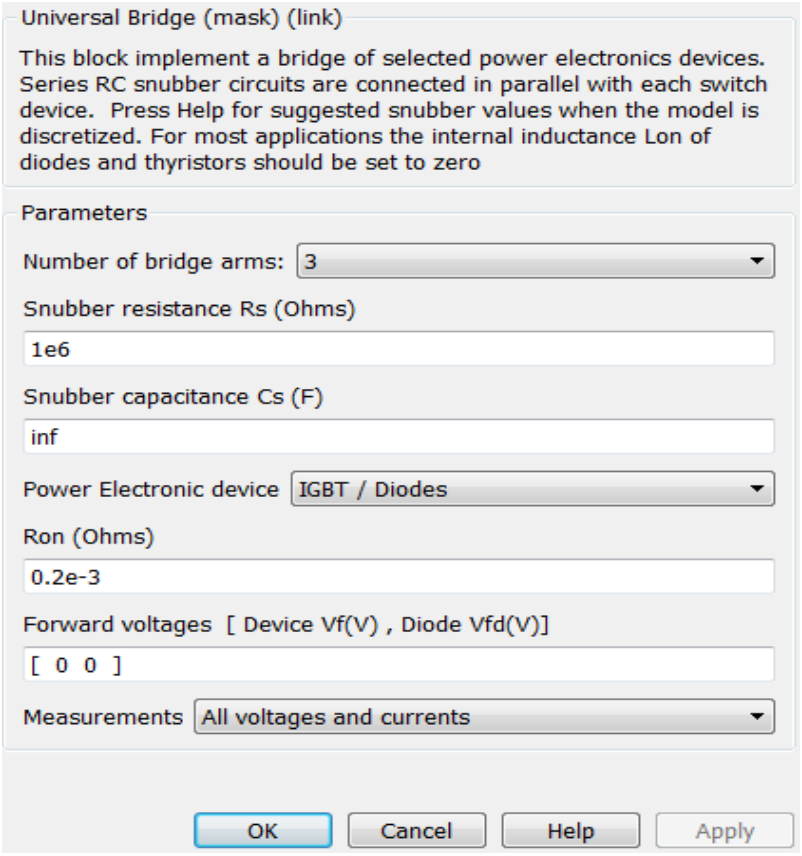

Figure 3.7: Inverter block settings

The gate pulse for the inverter are supplied using a pulse width modulation generator block, for which the settings are as shown in the fig. 3.8.

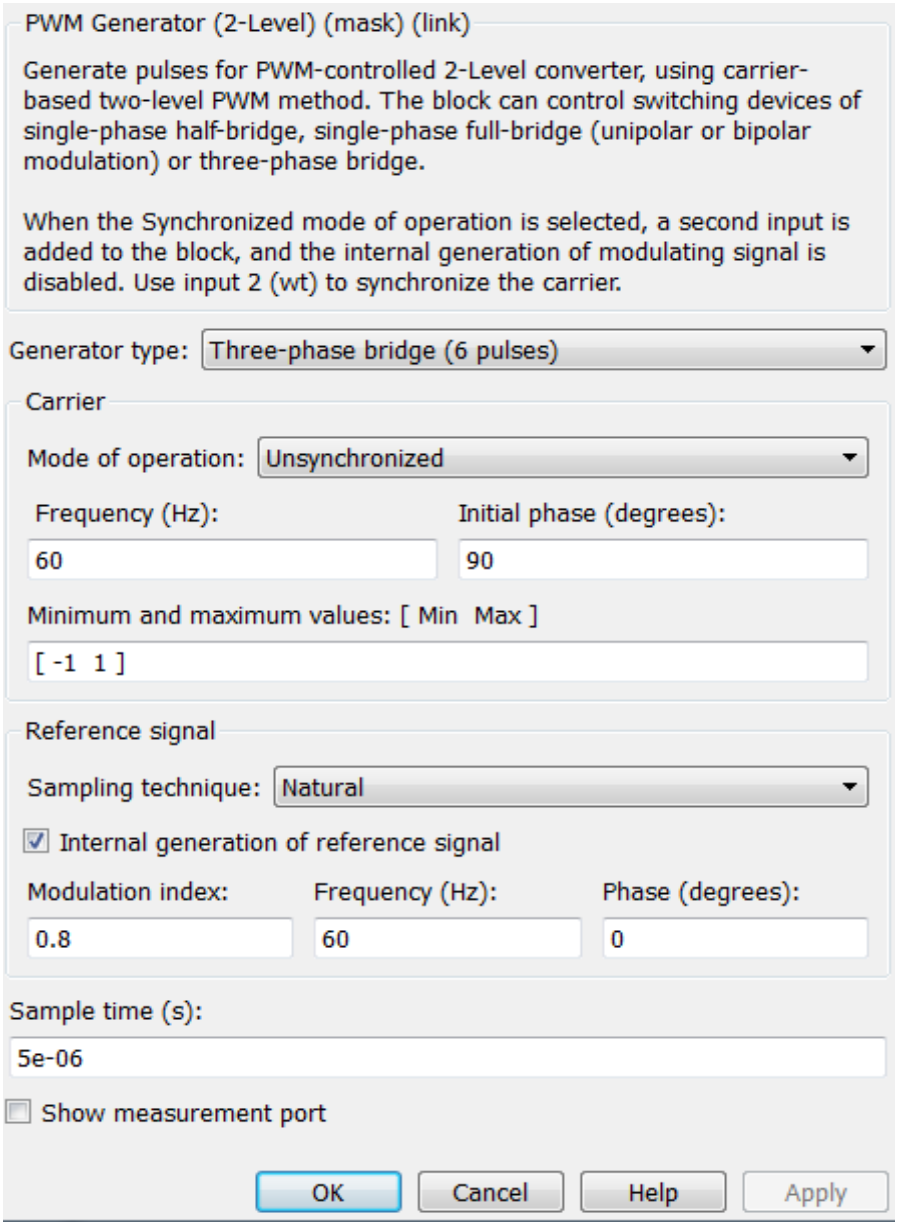

Figure 3.8: PWM generator block settings

3.5 IEEE 15 Bus System

The IEEE 15 bus test system provides the prefect simulation environment for a grid model. The system consists of an AC source operating as the swing bus. The line resistance and loads at each of the 15 buses are given in the appendix-1 [4]. The fig. 3.9 shows the IEEE 15 bus system, with the per unit voltages at each of the buses, after performing a load flow.

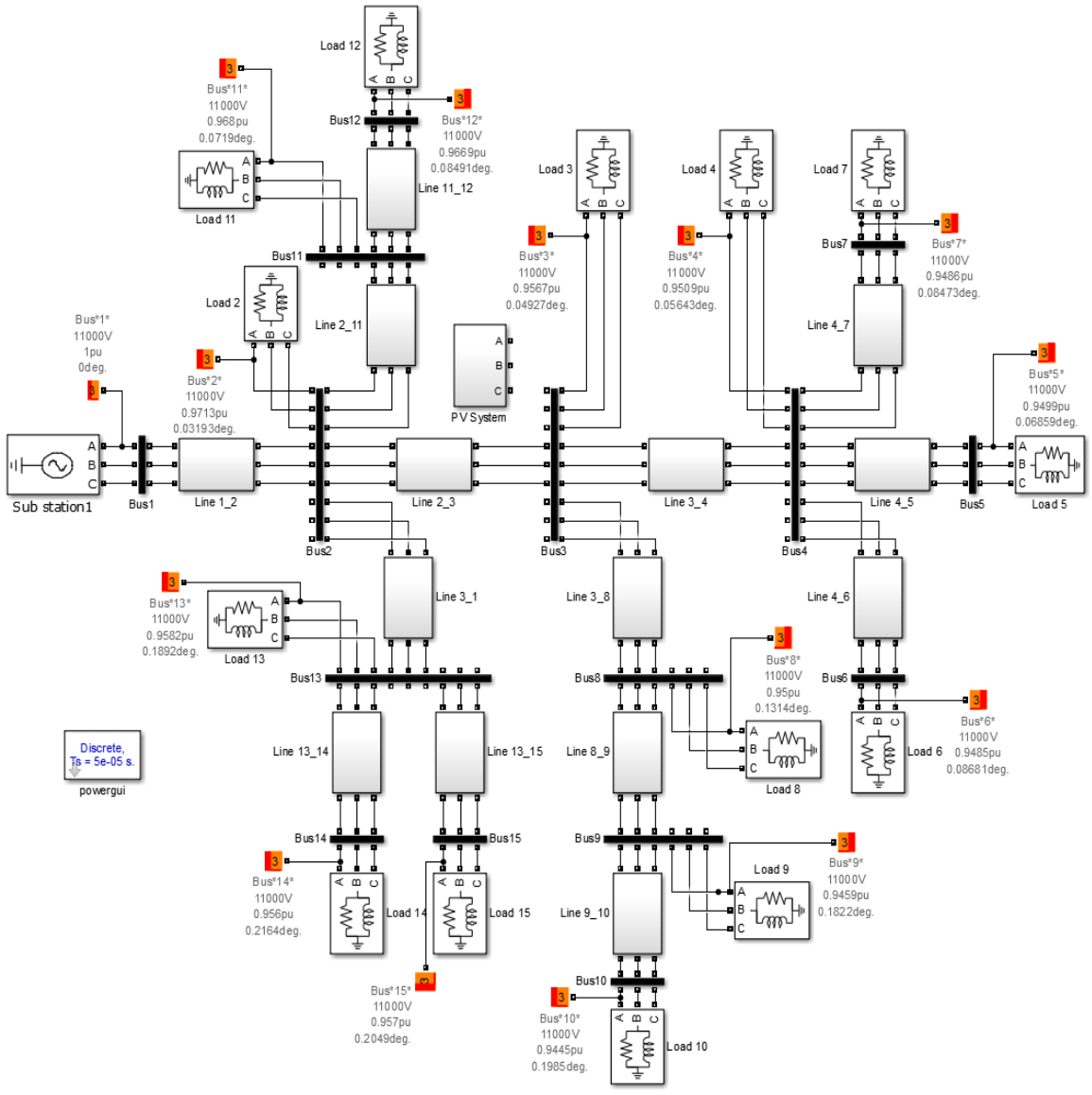

Figure 3.9: IEEE 15 Bus Test System

Chapter 4

Simulation Results

4.1 PV Panel Characteristics

The V-I, P-V curves for different insolation (1, 0.8, 0.6, 0.2 kW/m^2) and temperatures (25, 50, 75, 100 ^{o}C) respectively are as shown in the figures 4.1, 4.2, 4.3, 4.4.

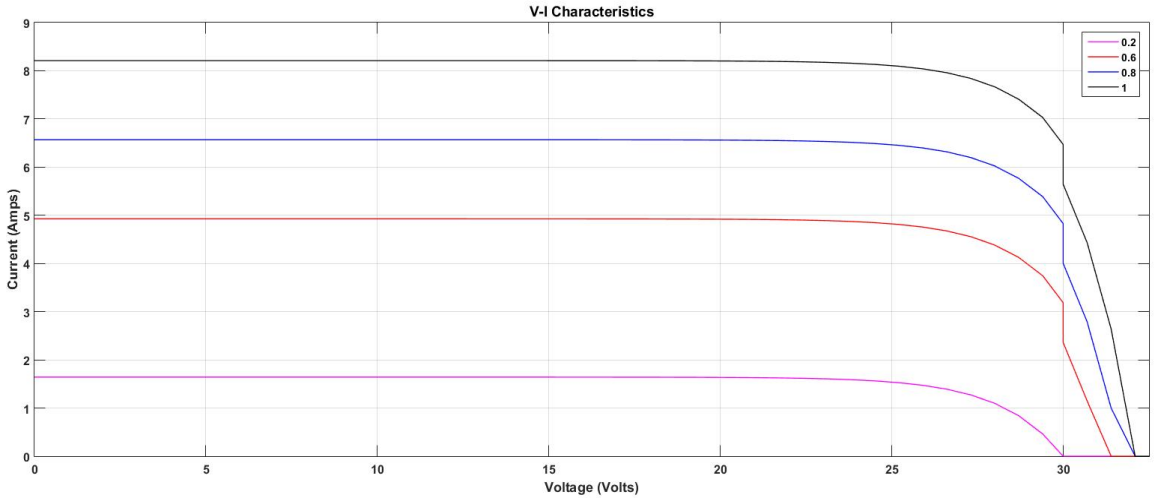

Figure 4.1: V-I Characteristics at varying insolation levels at 25^{o}Celsius

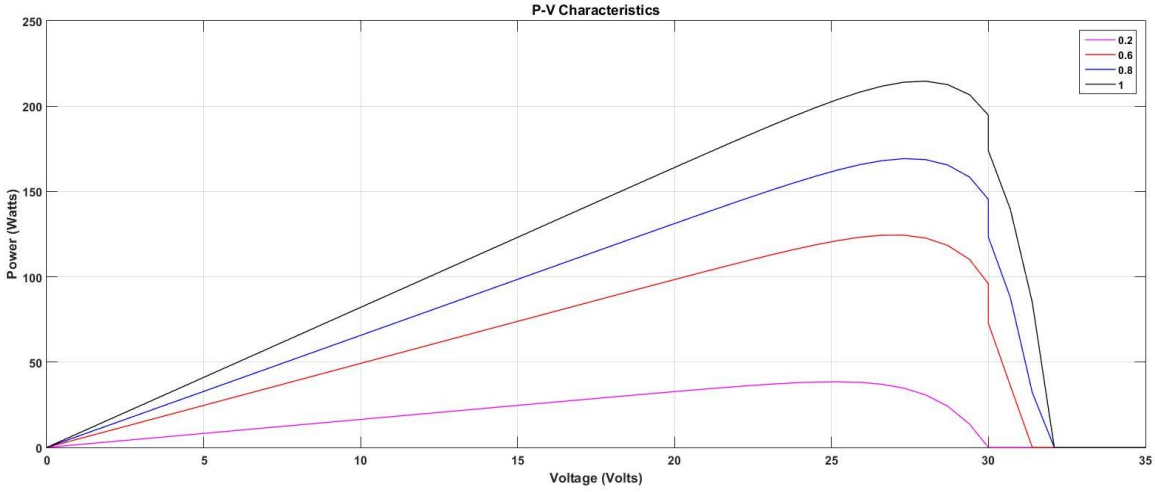

Figure 4.2: P-V Characteristics at varying insolation levels at 25^{o}Celsius

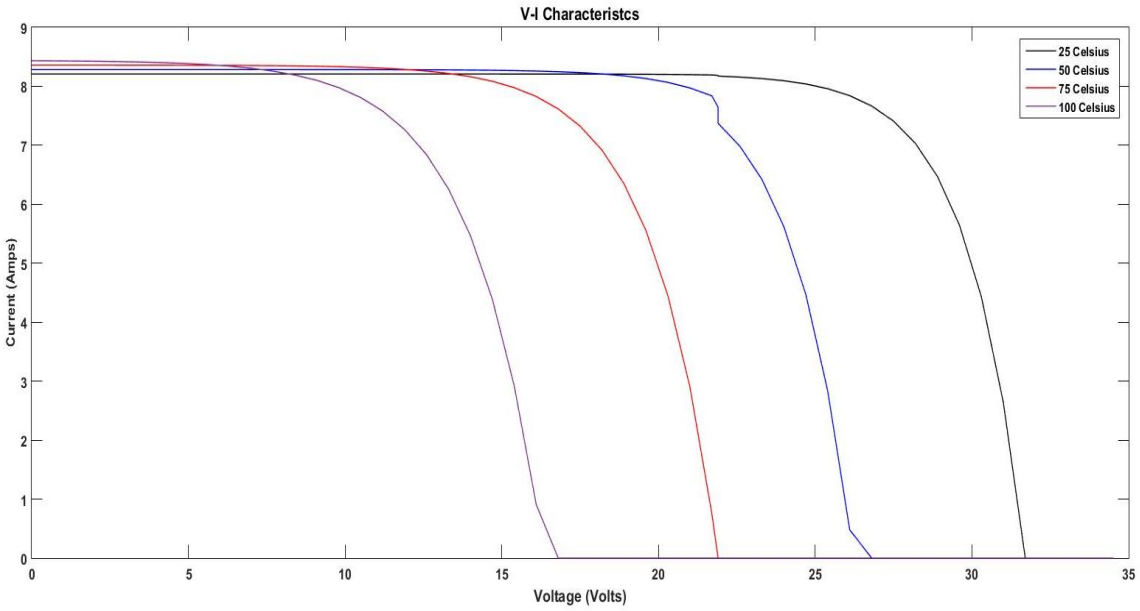

Figure 4.3: V-I Characteristics for varying temperatures at an insolation of 1 kW/m^2

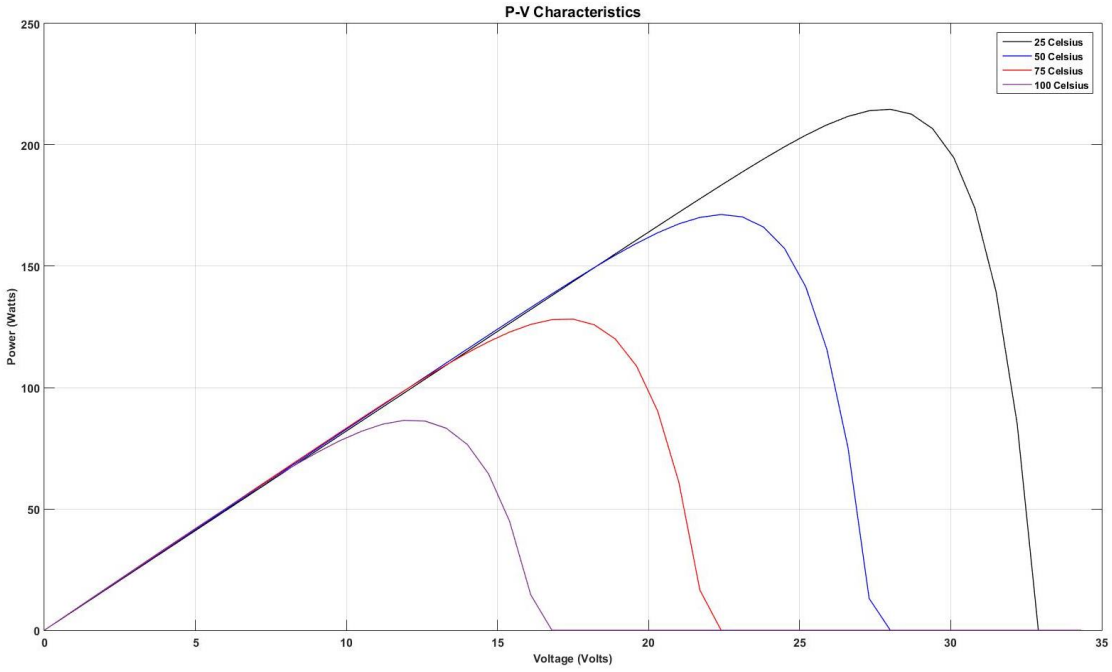

Figure 4.4: P-V Characteristics for varying temperatures at an insolation of 1 kW/m^2

4.2 PV System output

With the solar insolation and temperature input for Northridge, California as shown in fig. 3.4, the DC power output, voltage and current of the PV system is as shown in the figs. 4.5, 4.6 and 4.7 respectively.

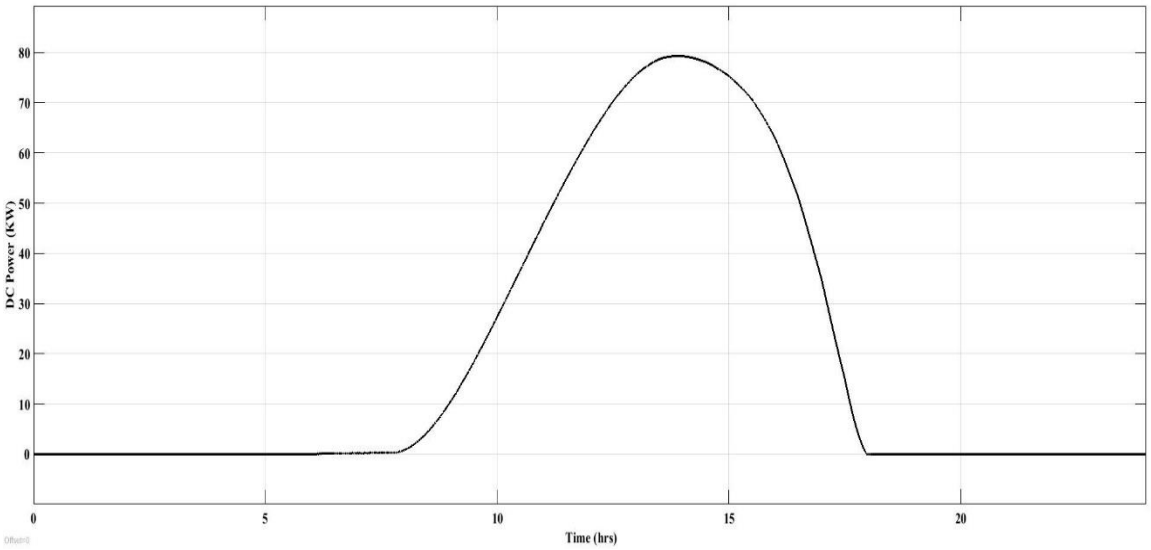

Figure 4.5: PV DC Power output

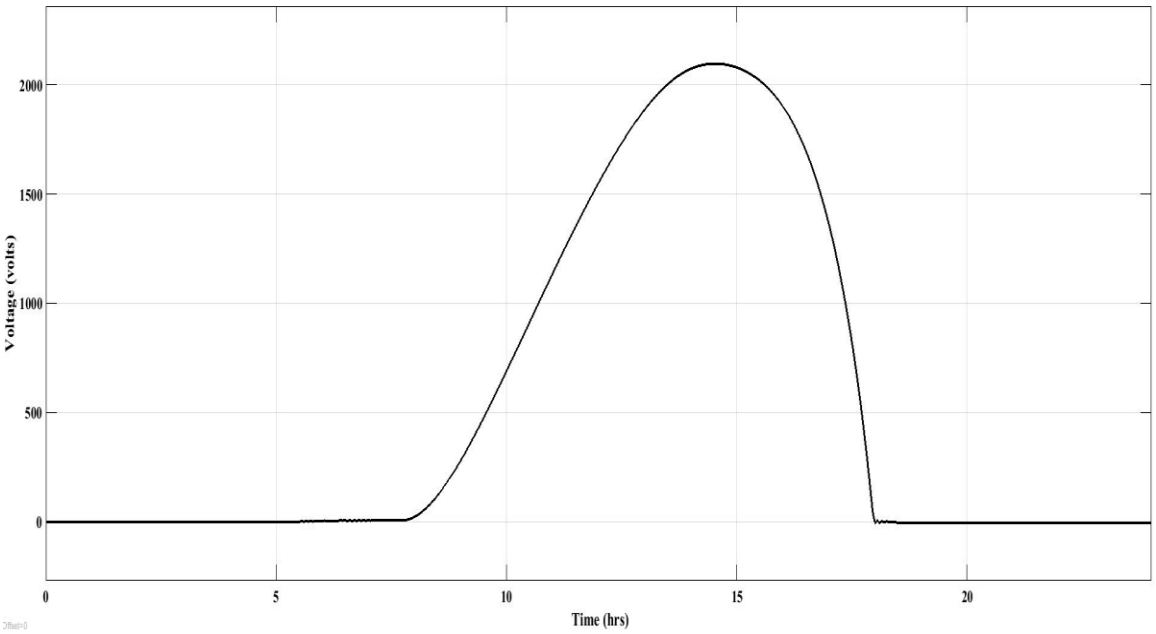

Figure 4.6: PV DC Voltage

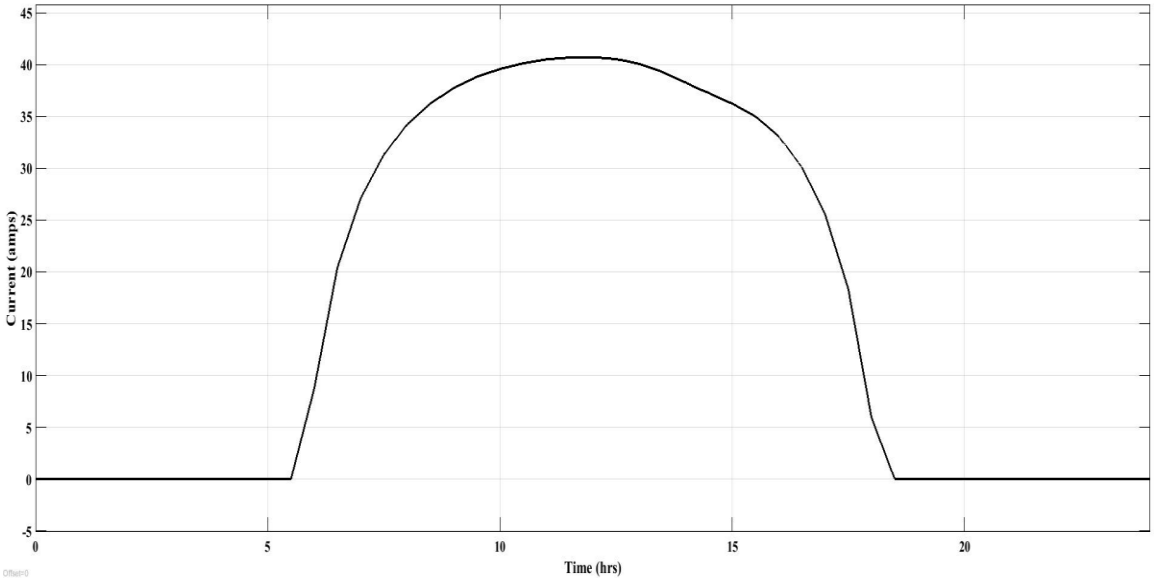

Figure 4.7: PV DC Current

The DC power generated by the PV system is converted to three phase AC using an inverter, the AC power measured at the HV side of the transformer is as shown in the fig. 4.8.

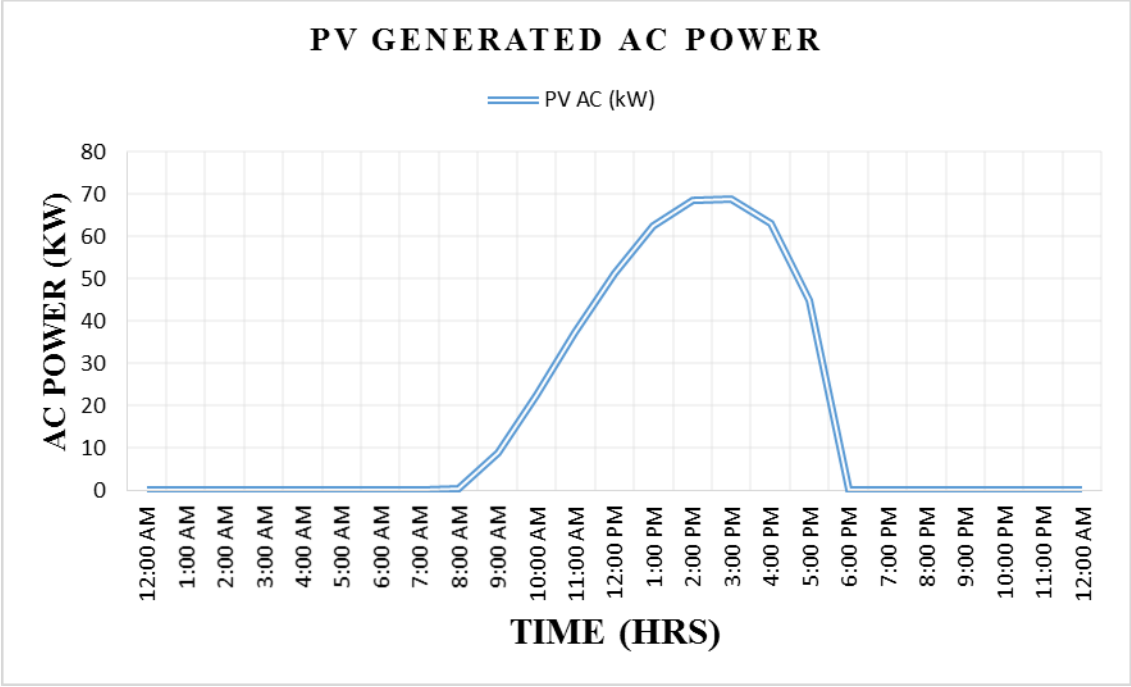

Figure 4.8: AC Power generated by PV

4.3 PV System connected to grid

Now, the PV system is connected to an IEEE 15 bus system as shown in the fig. 4.9, which acts as the grid, and the output difference with the PV connected and without the PV is plotted and described. The PV output curve is obtained for a typical day for the Northridge, California area. The substation acts as the swing bus for supply to the entire grid/IEEE 15 bus system.

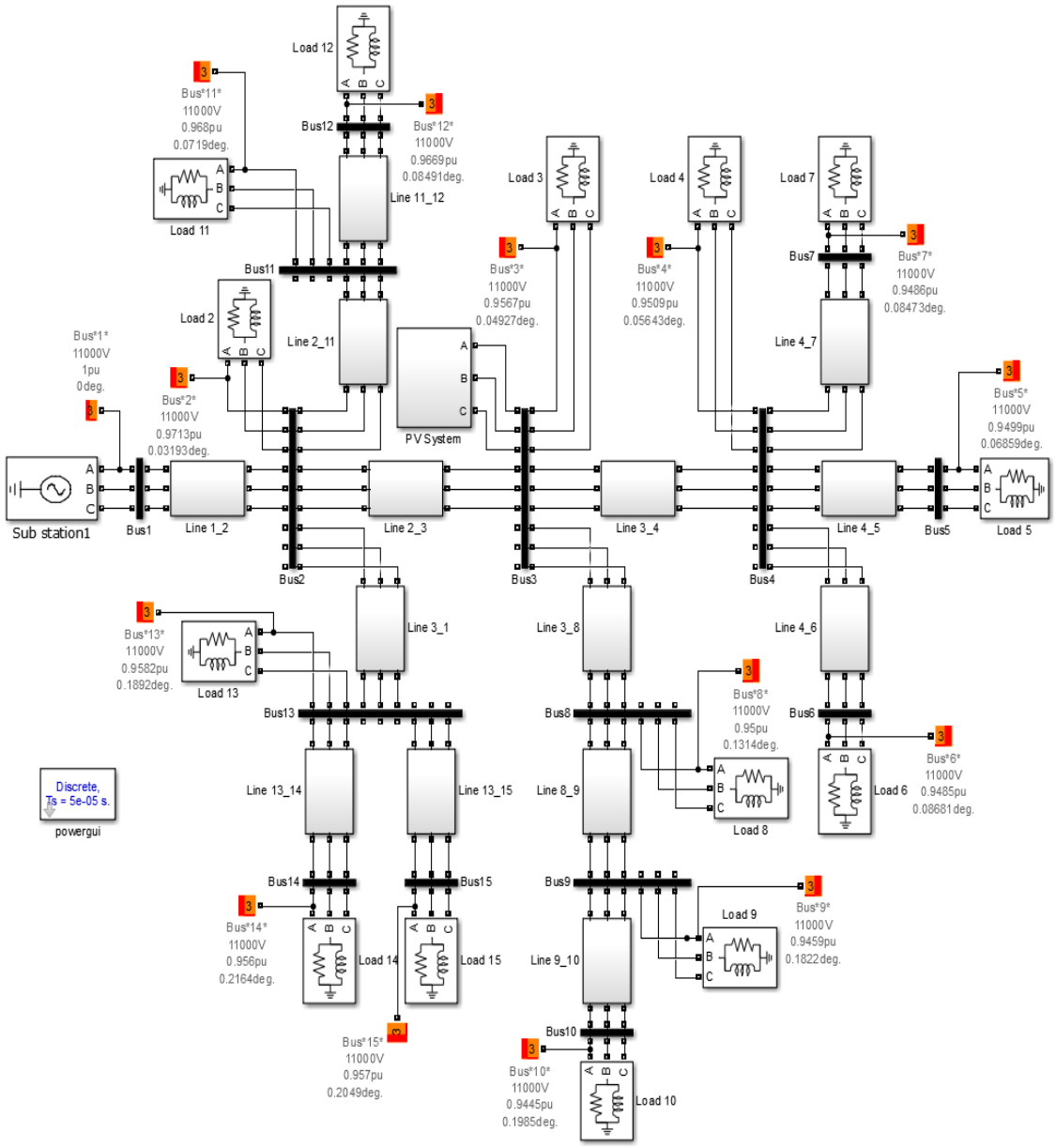

Figure 4.9 Photovoltaic system connected to the grid

The load flow analysis is carried out for two cases with different DG penetration levels: Case(I) 5%; Case(II) 10%

Case (I): DG penetration level = 5%

The fig. 4.10 shows the power supplied by the grid at each hour during a typical day, with and without a PV feeding the grid which is connected at the bus 3. The average power supplied by the grid is largely reduced, approx. 70kW when the PV output is maximum between 1PM to 2PM during the day.

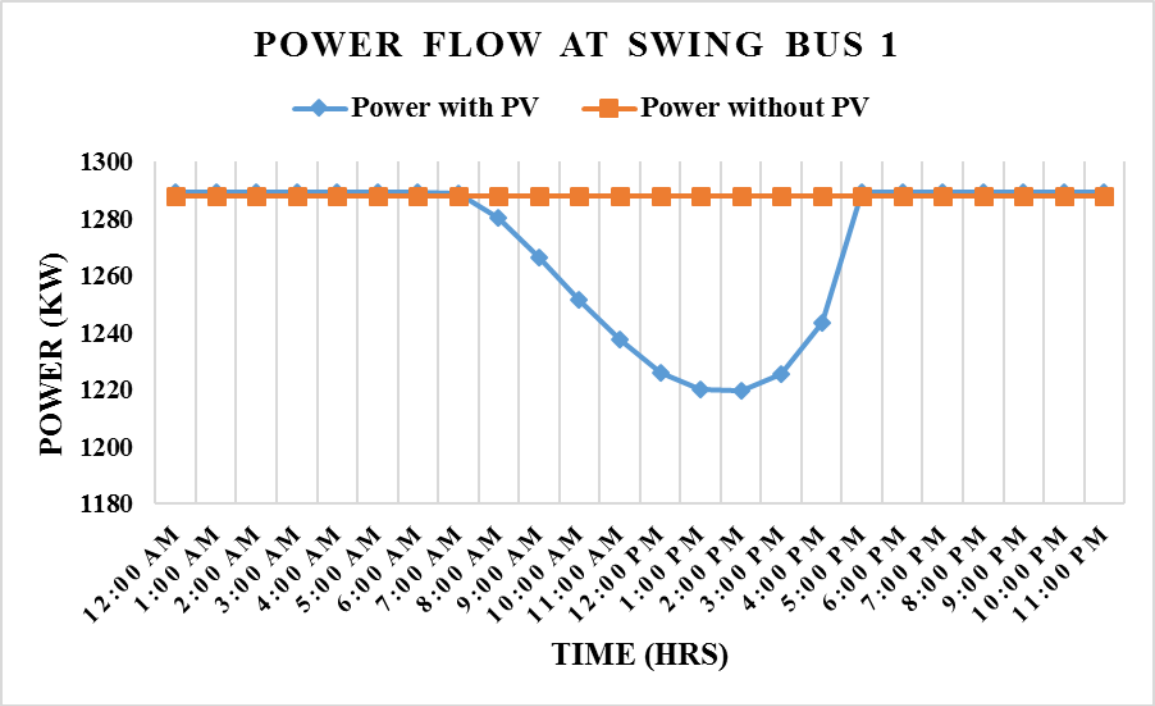

Figure 4.10: Power flow at swing bus with and without PV for Case(I)

The fig. 4.11 represents the voltage profile of the system without the PV. The voltage profile is constant at all the times.

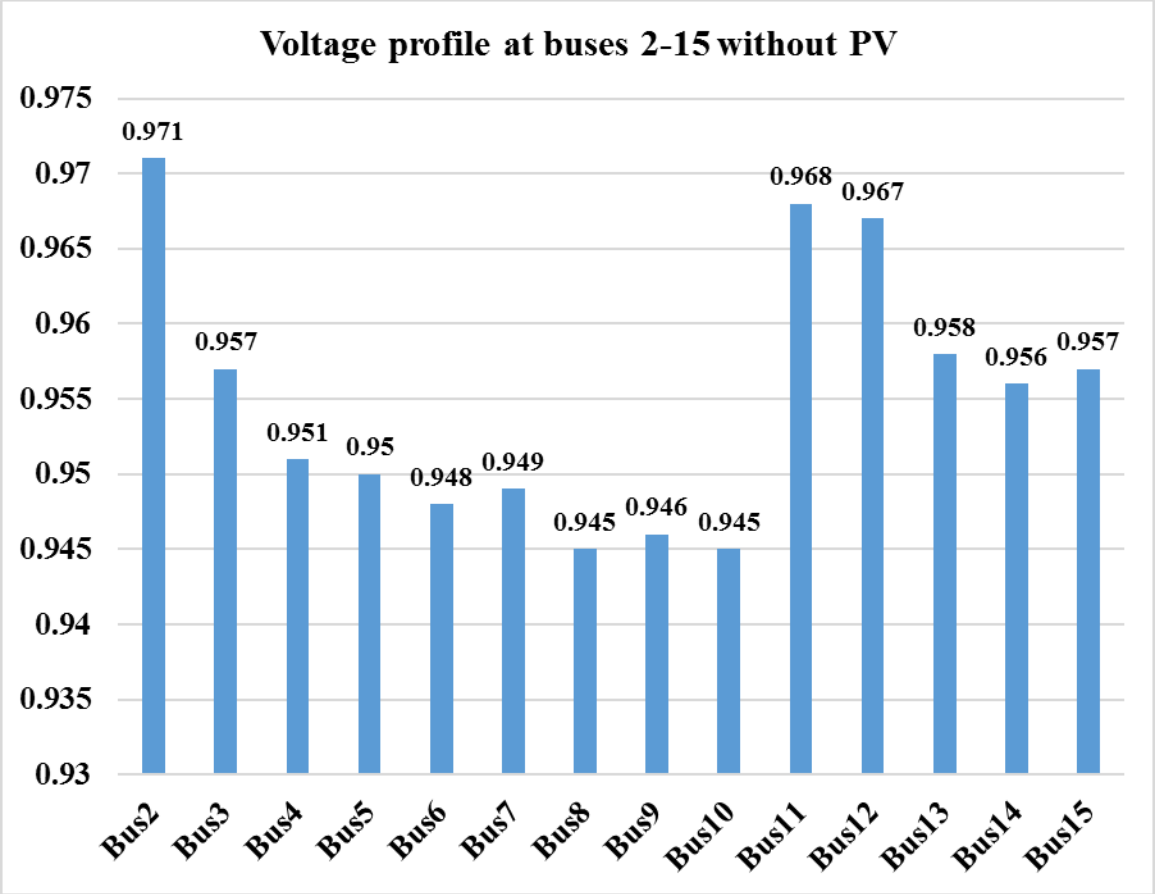

Figure 4.11: Voltage profile at buses 2-8 with PV connected at bus 3 for Case(I)

From the figs. 4.12 and 4.13, it can be clearly observed that the voltage profile of the system improves with the increase in power injected by the PV system into the grid.

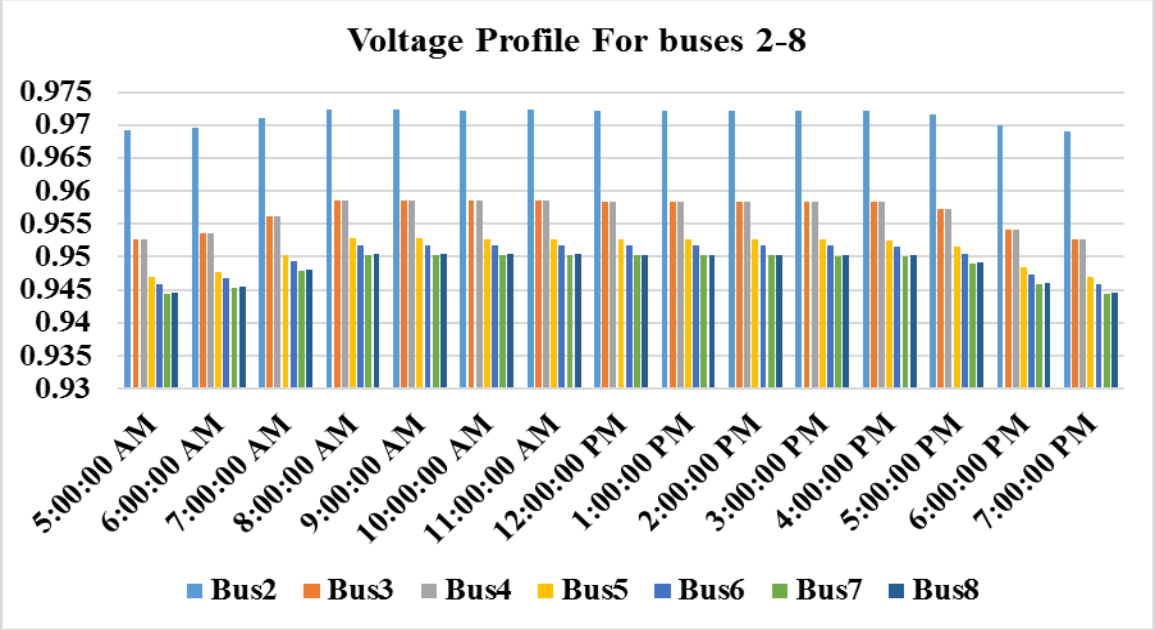

Figure 4.12: Voltage profile at buses 2-8 with PV connected at bus 3 for Case(I)

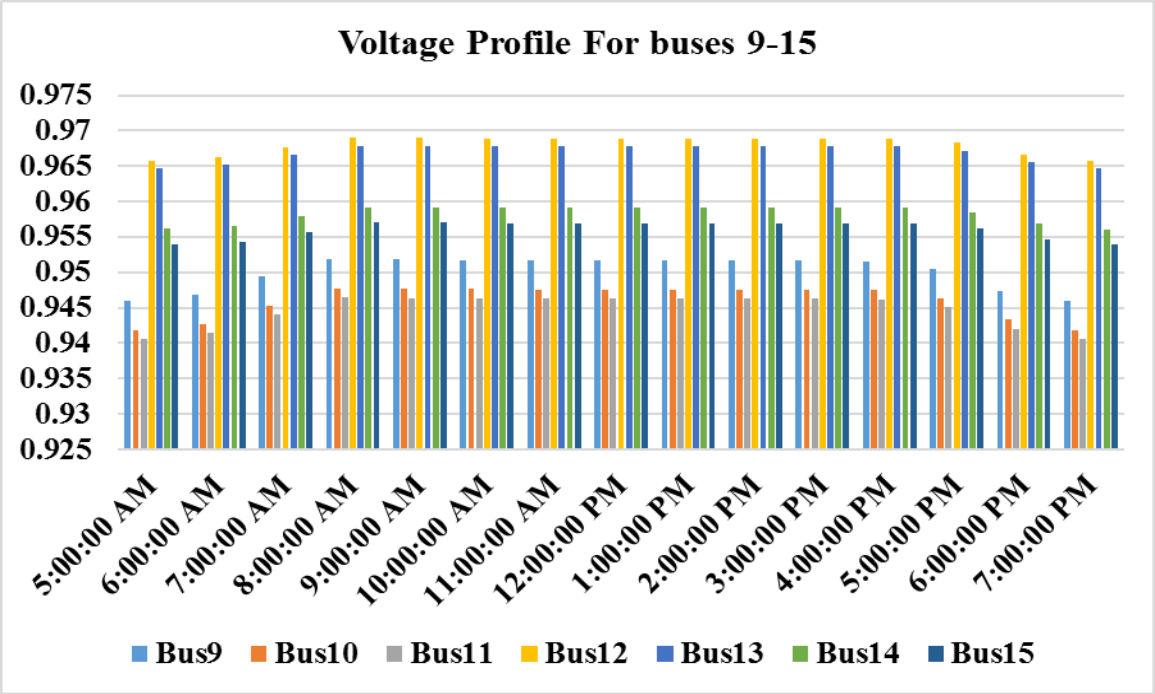

Figure 4.13: Voltage profile at buses 9-15 with PV connected at bus 3 for Case(I)

The fig. 4.14 and 4.15 represent the active and reactive power losses in the system with and without the PV.

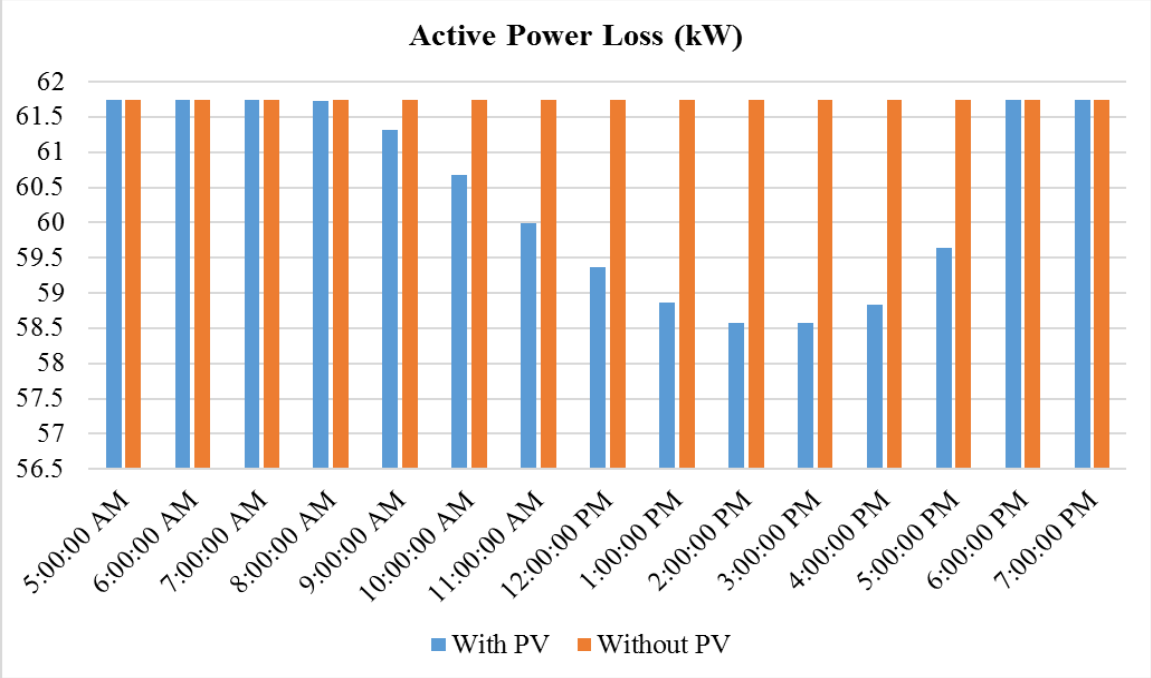

Figure 4.14: Comparison of Active Power Loss with and without PV for Case(I)

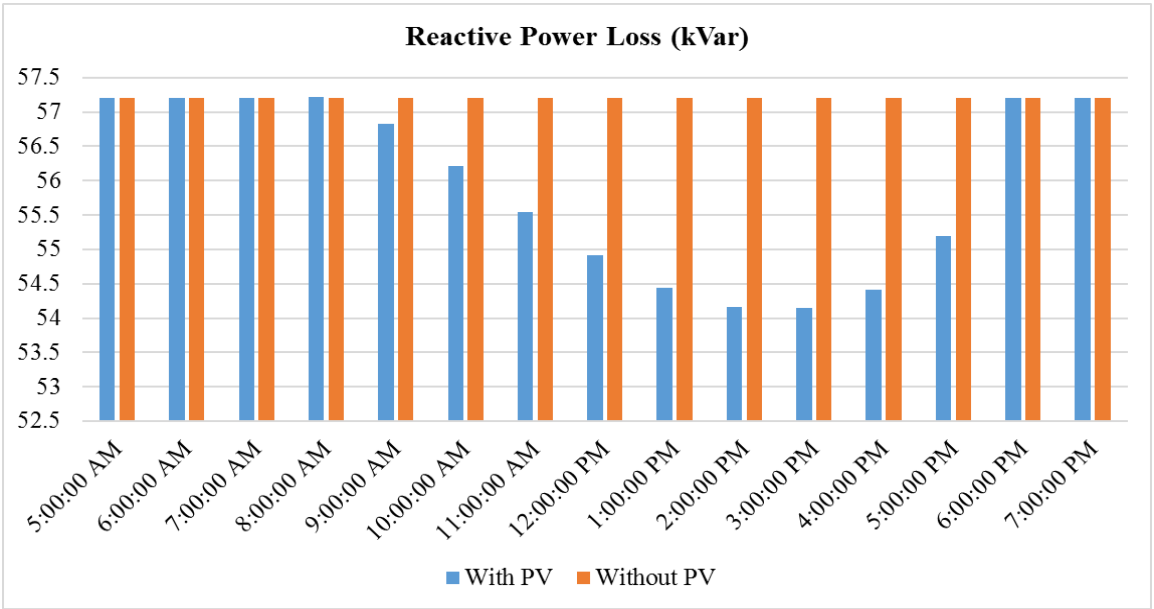

Figure 4.15: Comparison of Reactive Power Loss with and without PV for Case(I)

Case(II): DG penetration level = 10%

The DG penetration in Case(II) is 10% i.e. 120kW(approx..), which can be clearly observed from the fig. 4.16.

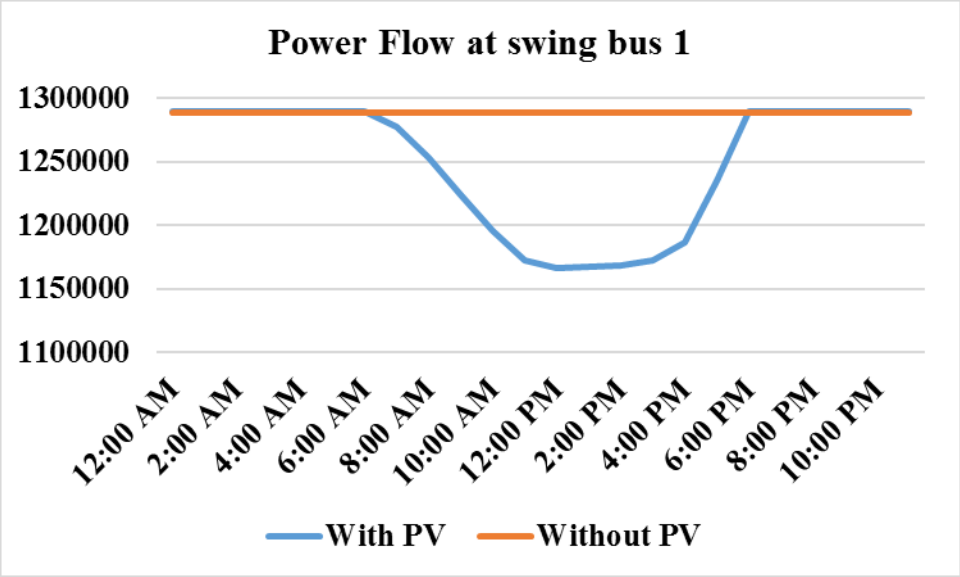

Figure 4.16: Power flow at swing bus with and without PV for Case(II)

The figs. 4.17, 4.18 show an improvement in the voltage profile of the system with increase in DG penetration.

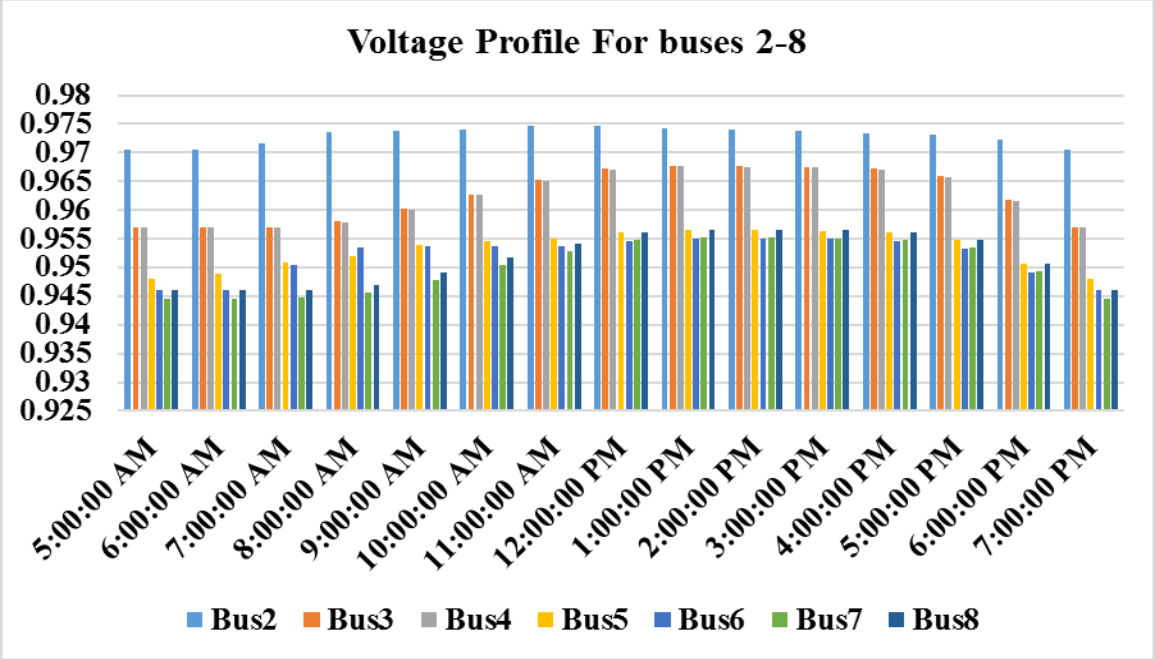

Figure 4.17: Voltage profile at buses 2-8 with PV connected at bus 3 for Case(II)

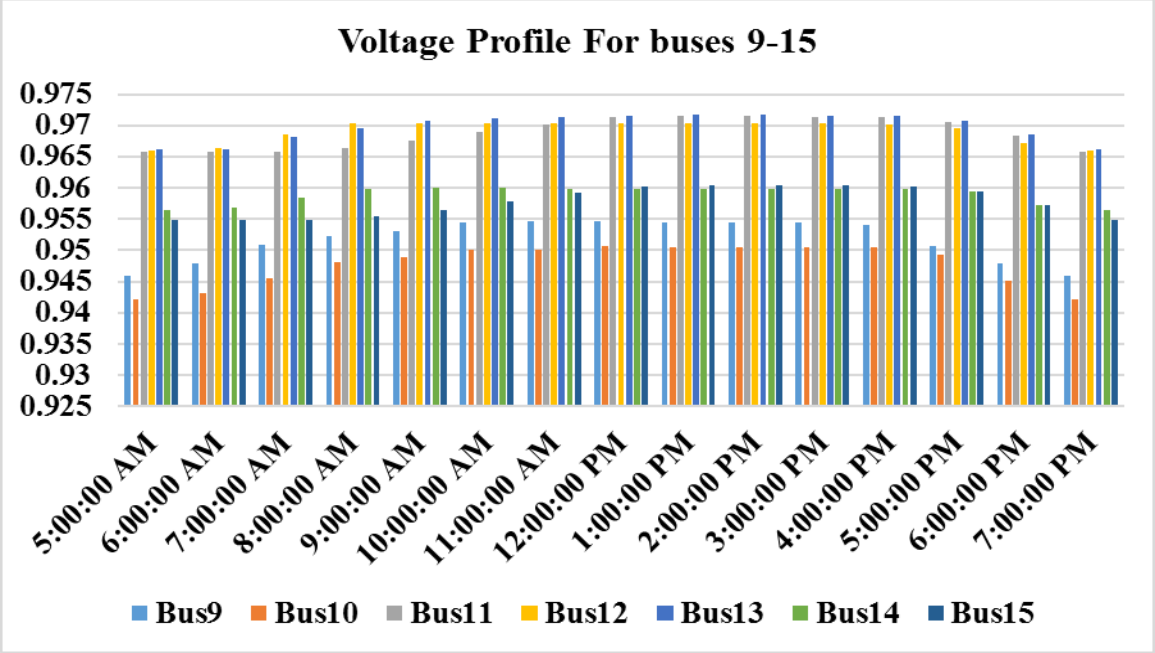

Figure 4.18: Voltage profile at buses 9-15 with PV connected at bus 3 for Case(II)

The figs. 4.19, 4.20 show the decrease in active and reactive power losses in the system, with increase in the DG penetration level.

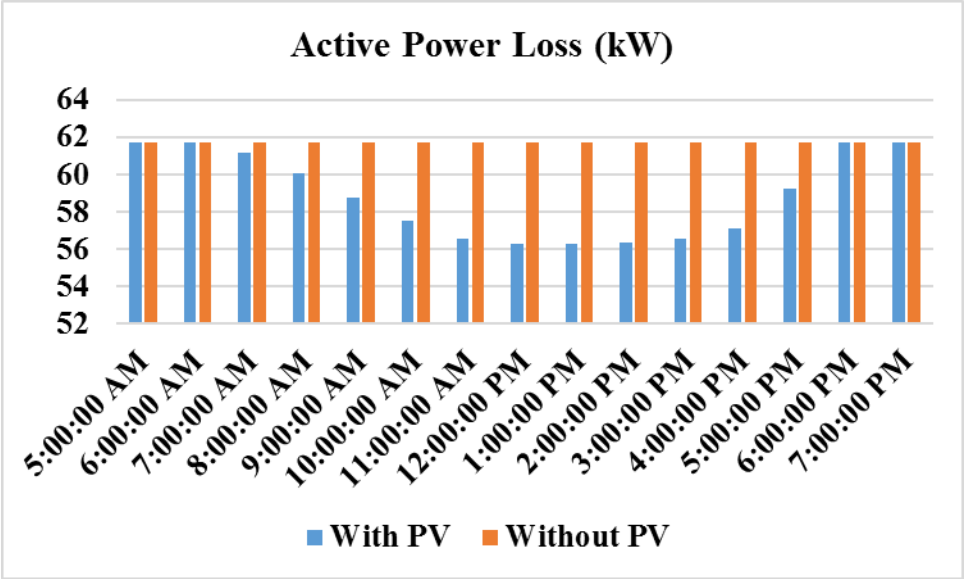

Figure 4.19: Comparison of Active Power Loss with and without PV for Case(II)

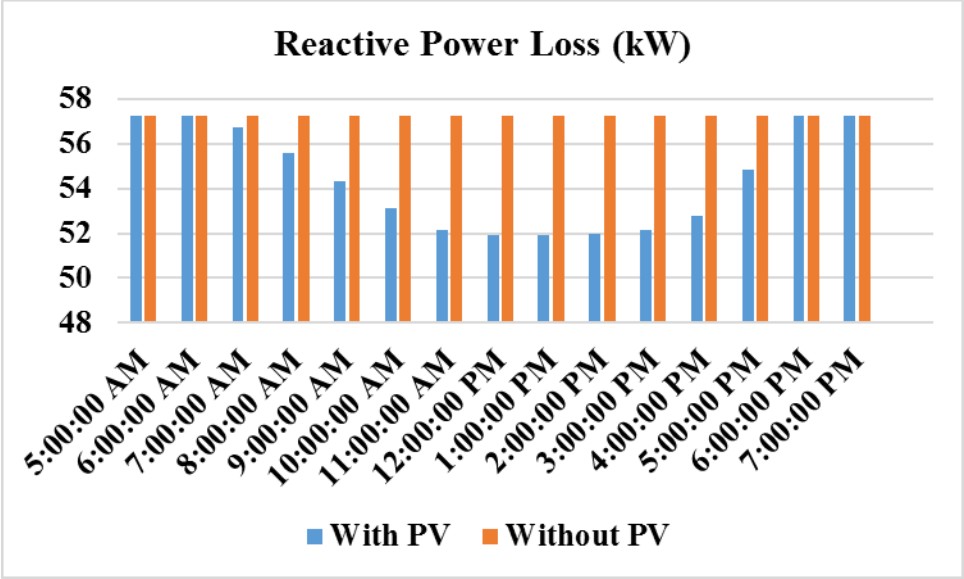

Figure 4.20: Comparison of Reactive Power Loss with and without PV for Case(II)

Comparison of Cases(I) & (II):

The fig. 4.21 shows the improvement in the voltage profile of the system with the increase in DG penetration from 5% to 10%.

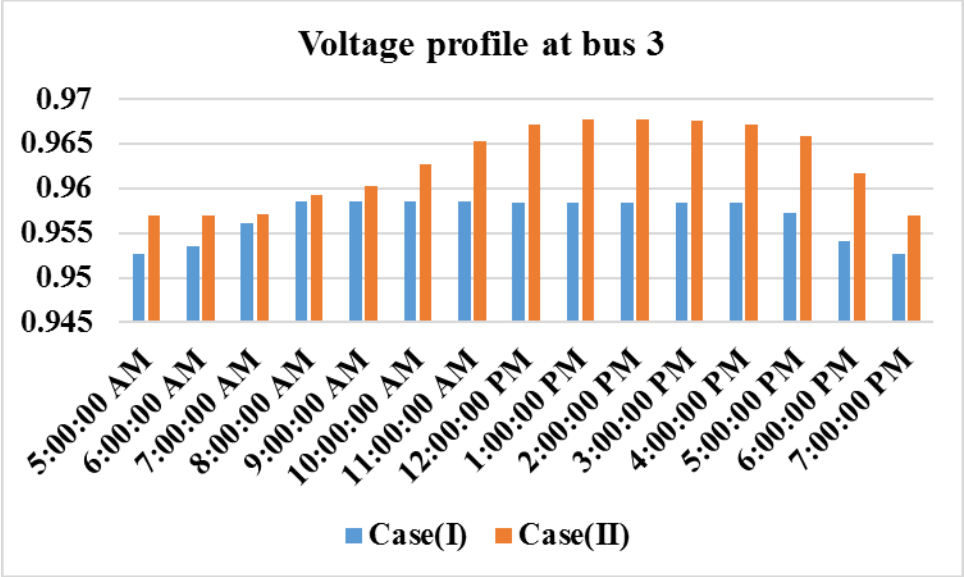

Figure 4.21: Comparison of voltage profiles for cases (I) & (II)

The figs. 4.22, 4.23 show the improvement in active and reactive power loss in the system when the DG penetration level is increased.

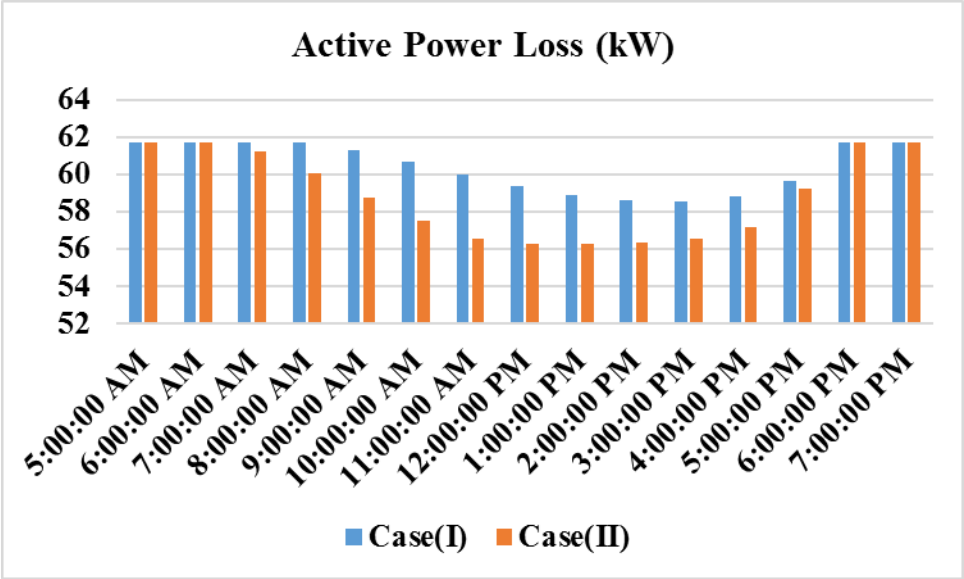

Figure 4.22: Comparison of Active Power Loss for cases (I) & (II)

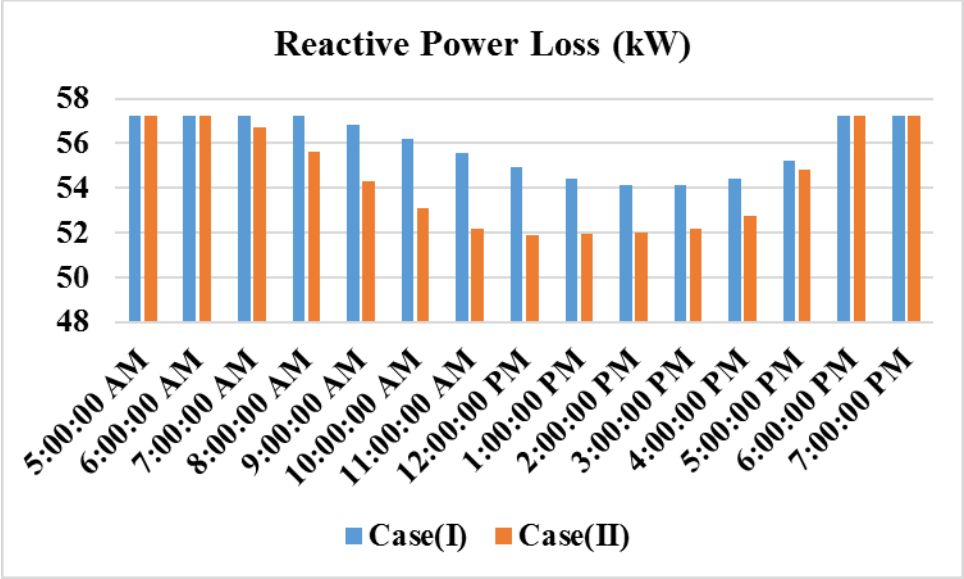

Figure 4.23: Comparison of Reactive Power Loss for cases (I) & (II)

Conclusion

Power generated by the PV increases slowly during the day as the solar insolation increases, and decreases as the sun sets or in the event of a passing cloud which can reduce the amount of solar radiation striking the surface of the PV panel.

The power delivered by the PV system during the day aids the substation/swing bus to supply the loads and reduce the burden on the grid generating station/substation. And apart from this the voltage profile of the power system is also improved, with the increase in the penetration level of the DG.

The active and reactive losses in the system are reduced as the power generated by the PV is close to the load and therefore the transmission losses are reduced [13].

However, before connecting a DG to the grid careful study must be conducted to ensure that there are no cases of over voltage when the solar irradiance is at the maximum on a sunny day. And also the protection systems must be adjusted for the effective operation of the grid when the distributed generation source starts generating power [8]. In addition to these the location, capacity, connection type and the number of DG's must be studied before connecting to the grid [9].

Appendix-1

Data for a 15-bus system

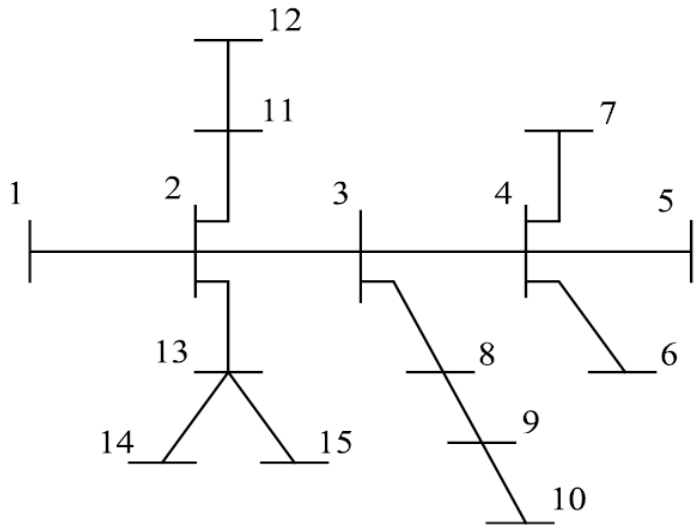

Figure 5.1: Single Line Diagram of an IEEE 15 bus system [4]

Sending node	Receiving node	r (ohm)	x (ohm)
1	2	1.35309	1.32349
2	3	1.17024	1.14464
3	4	0.84111	0.82271
4	5	1.52348	1.02760
4	6	1.19702	0.80740
4	7	2.23081	1.50470
3	8	1.79553	1.21110
8	9	2.44845	1.65150
9	10	2.01317	1.35790
2	11	2.01317	1.35790
11	12	1.68671	1.13770
2	13	2.55727	1.72490
13	14	1.08820	0.73400
13	15	1.25143	0.84410

Table 5.1: Line data of IEEE 15 bus system [4]

Appendix-2

Solar insolation data

Source	Location ID	City	State	Country	Latitude	Longitude
NSRDB	187528	Los Angels	CA	USA	34.33	-118.46
Year	Month	Day	Hour	Minute	DNI (W/m^2)	Temperature (^oC)
2015	4	2	0	0	0	9.56966553
2015	4	2	0	30	0	9.34243164
2015	4	2	1	0	0	9.11519775
2015	4	2	1	30	0	8.97197876
2015	4	2	2	0	0	8.82875977
2015	4	2	2	30	0	8.67128906
2015	4	2	3	0	0	8.51381836
2015	4	2	3	30	0	8.33120117
2015	4	2	4	0	0	8.14855347
2015	4	2	4	30	0	7.97322998
2015	4	2	5	0	0	7.79790649
2015	4	2	5	30	0	8.51656494
2015	4	2	6	0	214	9.23522339
2015	4	2	6	30	500	10.9171692
2015	4	2	7	0	663	12.599115
2015	4	2	7	30	766	14.3593079
2015	4	2	8	0	836	16.1195007
2015	4	2	8	30	885	17.6745544
2015	4	2	9	0	921	19.2295776
2015	4	2	9	30	947	20.6063477
2015	4	2	10	0	965	21.9831177
2015	4	2	10	30	978	23.0804077
2015	4	2	11	0	987	24.1777283

2015	4	2	11	30	991	24.9088684
2015	4	2	12	0	992	25.6400085
2015	4	2	12	30	989	25.8602234
2015	4	2	13	0	982	26.0804382
2015	4	2	13	30	971	25.9474426
2015	4	2	14	0	955	25.8144165
2015	4	2	14	30	933	25.2931152
2015	4	2	15	0	904	24.771814
2015	4	2	15	30	865	23.8279053
2015	4	2	16	0	811	22.8839661
2015	4	2	16	30	735	21.242334
2015	4	2	17	0	624	19.6007019
2015	4	2	17	30	448	17.7356201
2015	4	2	18	0	145	15.8705383
2015	4	2	18	30	0	15.3830811
2015	4	2	19	0	0	14.8956543
2015	4	2	19	30	0	14.6470581
2015	4	2	20	0	0	14.3984924
2015	4	2	20	30	0	14.0935913
2015	4	2	21	0	0	13.7886902
2015	4	2	21	30	0	13.4531494
2015	4	2	22	0	0	13.1176086
2015	4	2	22	30	0	12.8407532
2015	4	2	23	0	0	12.5638672
2015	4	2	23	30	0	12.3055969

Table 5.2: Data of solar insolation & temperature for Northridge, CA on 2nd April, 2015 [6]

Appendix-3

PV Module Specifications

Specifications

Electrical Performance under Standard Test Conditions (*STC)	
Maximum Power (Pmax)	200W (+10%/−5%)
Maximum Power Voltage (Vmpp)	26.3V
Maximum Power Current (Impp)	7.61A
Open Circuit Voltage (Voc)	32.9V
Short Circuit Current (Isc)	8.21A
Max System Voltage	600V
Temperature Coefficient of Voc	-1.23×10^{-1} V/℃
Temperature Coefficient of Isc	3.18×10^{-3} A/℃

*STC : Irradiance 1000W/m², AM1.5 spectrum, module temperture 25℃

Electrical Performance at 800W/m², NOCT, AM1.5	
Maximum Power (Pmax)	142W
Maximum Power Voltage (Vmpp)	23.2V
Maximum Power Current (Impp)	6.13A
Open Circuit Voltage (Voc)	29.9V
Short Circuit Current (Isc)	6.62A

NOCT (Nominal Operating Cell Temperature) : 47℃

Cells	
Number per Module	54

Module Characteristics	
Length × Width × Depth	1425mm(56.2in)×990mm(39.0in)×36mm(1.4in)
Weight	18.5kg(40.7lbs.)
Cable	(+)720mm(28.3in),(-)1800mm(70.9in)

Junction Box Characteristics	
Length × Width × Depth	113.6mm(4.5in)×76mm(3.0in)×9mm(0.4in)
IP Code	IP65

Reduction of Efficiency under Low Irradiance	
Reduction	7.8%

Reduction of efficiency from an irrandiance of 1000W/m² to 200W/m² (module temperature 25℃)

Figure 5.2: Kyocera KC200GT PV Module Specifications [11]

Bibliography

1. U.S. Energy Information Administration, https://www.eia.gov/ (2016, October 28)

2. Lighting Research Center, “Working of Photovoltaic Panels” (2016, October 30)

3. Yi-Jie Su, C.T. Huan-Liang Tsai, "Development of Generalized PV Model Using MATLAB/SIMULINK", Engineering and Computer Science World Congress 2008, SFO, USA, 2008

4. Singh, M, Panigrahi, B.K, Abhynkar, A.R, Mukherjee, R, Kundu, R, “Optimal location, size and protection coordination of distributed generation in distribution network”, IEEE Symposium on Swarm Intelligence, 2013

5. Mathworks example model, “Detailed model of a 100kw grid connected PV array”

6. Solar insolation map, http://www.nrel.gov/rredc (2016, August 25)

7. Chowdhury, Rahanuma Nireen Ali, Mohammed Mahedi Hasan, Md. Sarwar Uddin, Saiful Islam Rasel “Design & Simulation of Grid Connected Photovoltaic System using Simulink”, 3rd International Conference on Advances in EE, December, 2015, Bangladesh

8. R. Cheung, H. Cheung, L. Wang, A. Hamlyn, C.Yang, “Investigations of impacts of distributed generations on feeder protections,” IEEE P&E Society Gen. Meet., 2009

9. C.L Borges & D.M. Falcao, “Impact of DG allocation and sizing on reliability, losses and voltage profile,” IEEE Power Technology Conference, Italy, 2003.

10. M. J Alam, K. M. Muttaqi, and D. Sutanto,” Mitigation of Rooftop Solar PV Impacts and Evening”, IEEE Trans. on Power Systems, Volume 28, No. 4, Nov. 2013

11. http://www.kyocerasolar.com/dealers/product-center/manuals/Manual_KC130-200GT.pdf (2016, August 25)

12. http://www.conserve-energy-future.com/category/solar-energy (2016, November 5)

13. J. A. Sa'ed, S. Favuzza, M.G. Ippolito, F. Massaro, "Verifying the effect of distributed generators on voltage profile, power losses and protection system in Radial distribution networks" 4th International conference on Power Engineering, Energy and Electrical drives, 2013